1.5 ON THE FLUX REPRESENTATION OF INTERNAL WAVE SPECTRAL TRANSPORTS

Kurt Polzin
Woods Hole Oceanographic Institution
MS#21, WHOI, Woods Hole, MA 02543

Abstract: Recent fine- and microstructure observations indicate enhanced finescale shear and strain in conjunction with bottom intensified turbulent dissipation above rough bathymetry. Such observations implicate the bottom boundary as an energy source for the finescale internal wave field. An attempt is made here to describe a *simple* model for the spatial evolution of finescale internal waves as they propagate away from a source. Nonlinearity is explicitly treated as a flux in the spectral domain and dissipation is implicitly viewed as the end result of nonlinear transfers to high wavenumber. A general formulation for the nonlinear transfers is discussed which conserves both energy and momentum. A specific formulation is given to these transfers which can be described as a relaxation to an equilibrium power law and a backscattering process.

1. Introduction

Recent studies have documented a dramatic pattern a spatial variability in the deep ocean internal wave field. Above smoothly sloping abyssal plains and continental rise regions, finescale (vertical wavelengths of 10's to 100's of meters) spectra are near the background levels associated with the empirical Garrett and Munk spectral model[1] (Toole *et al.,* 1994; Kunze and Sanford, 1996; Polzin *et al.*, 1997; Polzin, 1999). Levels of turbulent dissipation are also low there (Toole *et al.*, 1994; Polzin *et al.*, 1997) and return a diapycnal diffusivity which is small and approximately independent of depth, ($K \leq 0.1 \times 10^{-4}$ m^2 s^{-1}). Above rough topography associated with the Mid-Atlantic Ridge, levels of turbulent mixing are orders of magnitude larger and increase with depth. Spectral levels of the finescale wave field are an order of magnitude larger than in the background (GM) wave field, implicating internal wave breaking as the source of turbulent energy. Polzin *et al.* (1997) proposed that the elevated fine structure levels were associated with the local generation of an internal tide having horizontal scales which were characteristic of the bottom topographic roughness ($\lesssim$1000 m). The scattering of waves incident upon the roughness (including the internal tide reflected from the surface) may also contribute to the finescale wavefield.

The above mentioned data suggest, as an ultimate goal, attaining the capability to make an entirely theoretical prediction for the vertical profile of turbulent dissipation by modeling the spatial decay of the wavefield. A lot of effort has been expended by the atmospheric science community on this problem. The oceanic context, though, is a bit different in its emphasis than the atmospheric. In the atmospheric context, wave–mean flow interaction and the decrease of density with height play the most significant roles in determining the rate of momentum and energy deposition, with buoyancy scaling and nonlinear interactions being increasingly less prominant. In the ocean, the discussion is dominated by the role of nonlinearity: Modeling the spatial decay of the finescale wavefield and constructing an entirely theoretical prediction for the vertical profile of turbulent dissipation requires a representation of the spectral transports associated with nonlinear interactions between the waves. This note serves to advertise recent advances along these lines presented in Polzin (2001a,b). In the following, the role and treatment of nonlinearity in atmospheric spectra is discussed prior to a consideration of the oceanic problem.

*Corresponding Author Address: Kurt L. Polzin, Physical Oceanography, MS #21, Woods Hole Oceanographic Institution, Woods Hole, MA 02543.

[1]GM75, Garrett and Munk, 1975; GM76, Cairns and Williams, 1976; M81, Munk 1981

2. Atmospheric Spectra

Atmospheric internal wave energy spectra admit to a succinct generalization, being largely independent of space and time. Empirical models (VanZandt and Fritts 1989) describe a separable spectrum:

$$E(\mu,\omega,\phi) = E_0 A(\mu) B(\omega) \Phi(\phi) \qquad (1)$$

where $\mu = m/m_\#$ is a nondimensional vertical wavenumber with $m_\#$ characterizing the energy containing scale of the wavefield, ω is the instrinsic frequency and the ϕ spectrum quantifies the azimuthal orientation of the wavefield. The spectral amplitude is given by $E_0 = N^2/10\, m_\#^2$. The vertical wavenumber and frequency spectra are:

$$A(\mu) = A_0 \frac{\mu^s}{1+\mu^{s+t}}, \left[A_0 = \frac{(s+t)}{\pi} \sin\frac{\pi(s+1)}{(s+t)} \right] \qquad (2)$$

$$B(\omega) = B_0 \omega^{-p}, \left[B_0 = \frac{(p-1) f^{p-1}}{1-(f/N)^{p-1}} \right] \qquad (3)$$

where N and f are the buoyancy and Coriolis frequency, respectively, and power laws of $s = 1$, $t = 3$ and $p = 5/3$ are representative. Upward energy propagation at all vertical wavenumbers is generally assumed. The most universal aspect of this model is the high wavenumber portion of the spectrum.

Observed spectra tend toward a form of $\alpha\, N^2 m^{-3}$ at high wavenumber, with α being remarkably independent of time, space and meteorological conditions (*e.g.*, Dewan *et al.*, 1984; Wu and Widdel, 1991). Saturation arguments have been forwarded to explain this universality. These include linear instability (*e.g.*, Dewan and Good, 1986; Smith *et al.*, 1987) and Doppler shifting of small-scale waves by the horizontal velocities of larger scale waves (*e.g.*, Hines, 1993). The former implies the presence of

diabatic processes removing energy from waves having finite wavenumber. The later is one representation of non-linear adiabatic interactions between internal waves, conserving momentum and energy, but not, in general, action.

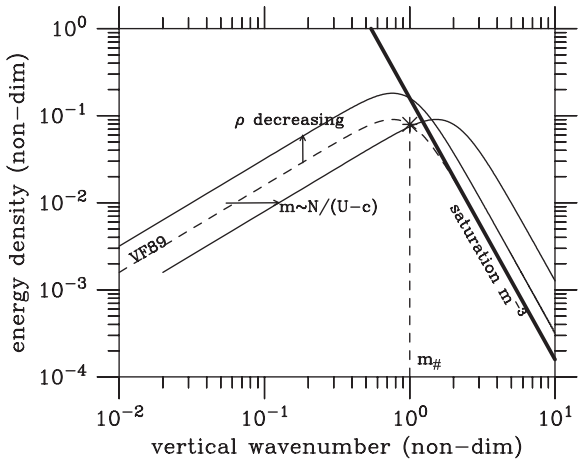

Figure 1. A schematic representation of the atmospheric shear spectrum. The dashed line denotes the VF89 spectrum with roll-off at $m_\#$ and m^{-3} saturation regime. The solid lines depict the evolution of the spectrum for decreasing density (shifted upwards) and increasing wavenumber associated with propagation into increasing startification or towards a critical layer.

Internal gravity waves represented by (1) [Figure 1] will evolve in response to changes in meteorological conditions. These can be assessed in the context of conservative, linear internal wave propagation. This implies the vertical wavenumber varies as:

$$m = N(z) / \left(U(z) - c\right) \tag{4}$$

where U is the background horizontal current and $c = \sigma/k$ is the horizontal phase speed relative to the ground. The spectral amplitude evolves such that the vertical flux of horizontal momuntum,

$$\rho < u'w' > = \rho C_{gz} E(m,\omega) k / \omega = \text{constant}, \tag{5}$$

where u' and w' are the perturbation velocities associated with the wavefield and C_{gz} is the vertical group velocity, is independent of height (the effects of rotation have been neglected for the sake of clarity in exposition). This later condition dictates how $E(m)$ varies in response to changes in m associated with changes in $N(z)$ or $U(z)$ and that $E(m)$ increases in proportion to decreases in ρ (Figure 1).

The issue is that this conservative, linear wave propagation often implies a transfer of energy to higher wavenumber and/or increase in amplitude so that the high wavenumber portion of the spectrum exceeds the saturation condition (Figure 1). In such instances either instability or nonlinearity is invoked to argue for a relaxation of the spectra back to a saturation line, with the excess energy considered to be transfered to smaller scales. In a practical sense, this means defining how one modifies (4) at $m_\#$ to account for saturation. Hines (1997) resolves this as

$$m_\# = N(z_0) / (U(z_0) - U(z) - \Gamma u'_{rms}) \tag{6}$$

where Γ is an $O(1)$ constant, u'_{rms} is estimated over $m \le m_\#$ and z_0 is a reference level. Fritts and Lu (1993) suggest:

$$m_\# = \left[\frac{N(z)}{N(z_0)}\right]^{3/4} \frac{\rho(z_0)}{\rho(z)} \frac{m_\#(z_0)}{1 - m_\#(z_0)/\hat{m}(z)} \tag{7}$$

with $\hat{m}(z) = N(z) / \left(U(z) - U(z_0)\right)$. One could, as well, apply linear instability criteria to individual elements of the spectrum (*e.g.,* Lindzen 1981).

3. Oceanic Spectra

Oceanic vertical wavenumber (m) spectra of shear (S_z) tend to exhibit a characteristic form depicted in Figure 2. The spectral shape for wavenumbers $m < m_c$ is the GM76 model: approximately white ($m_\# < m < m_c$) with magnitude obeying *WKB* scaling ($S_z \propto N^2$). At the lowest wavenumbers, the spectrum rolls off as $S_z \propto m^2/(m_\# + m)^2$, at a wavenumber $m_\# = 3\pi/1300$ m (N/N_0) equivalent to mode 3 (N_0 = 3 cph). The GM models make no reference to the background flow and while N^2 is highly variable, the density is constant to within 1%. The dynamical content of the GM models is limited to consistency with linear propagation and buoyancy scaling in the hydrostatic limit. The wavefield is considered to be horizontally isotropic and vertically symmetric: there is no preferred direction for wave propagation. It is also considered to be horizontally and temporally homogeneous, or in other words, universal. Consequently there are no sources, no sinks, nor any transfers of energy in either the spatial or frequency domain. The degree of agreement between these models and routine observations is astounding: deviations beyond a factor of 2 or 3 are rare. For comparison with (1), the GM model is:

$$E = E_0 b^2 N_0 N A(\mu) B(\omega) \tag{8}$$

$$A(\mu) = \frac{A_0}{(\mu + \mu_*)^2}, \left[A_0 = 1\right] \tag{9}$$

$$B(\omega) = \frac{B_0}{\omega\left(\omega^2 - f^2\right)^{1/2}}, \left[B_0 = \frac{2f}{\pi}\right] \tag{10}$$

with $E_0 = 6.3 \times 10^{-5}$, b = 1300 m and N_0=3 cph.

This is not to say, though, that the oceanic wavefield is entirely linear and inviscid. The uniform level of the shear spectrum (that is, $E(m) \propto m^{-2}$!) for vertical wavenumbers $m_\# < m \le m_c$ is believed to be set by self-interactions within the internal wavefield. Models of both resonant interactions and eikonal representations of wave–wave

interactions suggest that the uniform level of the GM76 and M81 shear spectra[2] is statistically stationary with

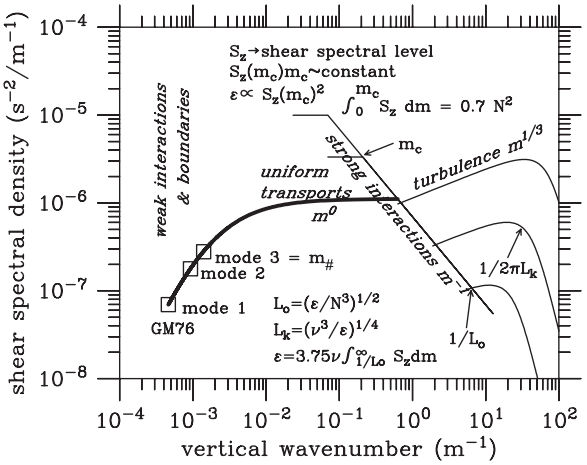

Figure 2. A schematic representation of the oceanic shear spectrum. The thick line denotes the GM76 spectrum with m^{-1} roll-off and associated turbulence spectrum. The turbulent shear spectrum assumes universal, isotropic turbulence. The partial spectra having cut-offs m_c at lower wavenumber are depicted with thin lines. The figure associates spectral levels $S(m_c)$ of 3 and 9 times the GM spectrum with dissipations 9 and 81 times larger. The spectral transition points are $m_\#$, m_c, $1/L_o$, and $1/L_k$.

respect to internal wave interactions. One way to gauge the strength of the non-linearity is to estimate the nonlinear time scale (τ_{trans}) from the wave frequency ω, turbulent dissipation ε associated with internal wave breaking and energy density $E(m)$:

$$\tau_{trans}(m) \times \omega = \omega \times mE(m)/\varepsilon \cong m/m_c \qquad (11)$$

where m_c is a cut-off wavenumber defined from the shear variance $[S^2(m)]$,

$$S^2(m_c) = 2\int_0^{m_c} m'^2 E_k(m')\, dm' = 0.7N^2 \qquad (12)$$

and it has been assumed that the downscale transport at m is equal to the dissipation rate. For the GM76 spectrum, m_c represents a 10-m vertical wavelength. In the abyssal Brazil Basin, $2\pi/m_c$ is approximately 100 m.

Beyond m_c, the spectrum falls as approximately m^{-1}. From an observational standpoint (Gargett *et al.,* 1981, Duda and Cox 1989, Gregg *et al.,* 1993), there is evidence that m_c is independent of N and varies inversely with the average shear spectral density of wavenumbers $m < m_c$. However, both Duda and Cox (1989) and Gregg *et al.,* 1993 point to quantitative exceptions. The m^{-1} region between m_c and L_o^{-1} corresponds to the atmospheric saturation range, albeit at a somewhat higher spectral level, with $E_{ocean}(m) \cong (1/2)\ N^2\ m^{-3}$ versus $E_{atmos}(m) \cong (2/5\pi)\ N^2\ m^{-3}$. My personal predilection is to interpret the roll-off m_c as being a response to increasing adiabatic non-linearity: Wave breaking associated with shear instability, for example, appears to be an important process only for wavenumbers $m > 2\ m_c$, Polzin (1996). Non-linearity thus appears to play a much more important role in shaping the oceanic internal wave spectrum and has thus received more detailed consideration in that context. The following describes an attempt to incorporate non-linearity explicitly into a propagation model.

[2]The GM75 spectrum specifies an $m^{-1/2}$ power law.

4. Conservation Statements

Consideration of the fluxes of energy through the faces of a kinematic box (Figure 3) in the spectral–spatial domain leads to the following energy balance:[3]

$$\frac{\partial E^{\pm}}{\partial t} \pm \frac{\partial \left[C_{gz}E^{\pm}\right]}{\partial z} + \frac{\partial F_e^{\pm}}{\partial m} + \frac{\partial G_e^{\pm}}{\partial \omega} = \left[S_o^{\pm} - S_i^{\pm}\right]_e, \qquad (13)$$

where $E^{\pm}(m,\omega,z,t)$ is the vertical wavenumber-frequency energy density of either the upward (+) or downward (–) propagating wavefield, $|C_{gz}| = (\omega^2 - f^2)(N^2 - \omega^2)/\omega\, m$ $(N^2 - f^2)$ is the vertical group velocity]; down-scale spectral transfers of energy are represented by $F_e^{\pm}(m,\omega,z,t)$; and spectral transfers in the frequency domain are given by $G_e^{\pm}(m,\omega,z,t)$.[4]

This equation defines the evolution of the vertical wavenumber-frequency energy density as a function of vertical coordinate and time. The fluxes $F_e^{\pm}(m,\omega)$ and $G_e^{\pm}(m,\omega)$ represent the transfer of wave energy in vertical wavenumber-frequency space associated with a variety of

physical mechanisms: wave–wave interactions, buoyancy scaling and wave–mean flow interactions. Of exclusive interest here are wave–wave interactions. The source-sink terms on the right hand side of (13) can represent either the production or dissipation of energy or the transfer of energy between waves having different wavenumber and frequency. The resonant interaction between members of a triad (*e.g.*, Müller *et al.,* 1986) is an example of the later. Only flux representations of wave–wave interactions are considered here. In the oceanic context, wave generation occurs at the boundaries (*e.g.*, internal tide generation or atmospheric forcing) and is best represented as a boundary value problem rather than as

[3]$E^{\pm}(m,\omega,z,t) \equiv E^{\pm}$ is the vertical wavenumber-frequency energy density with direction of energy propagation denoted by either + or –. The notation $E^{\pm}(m,z,t)$ [or $F^{\pm}(m,z,t)$] denotes integration over the frequency domain, $E^{\pm}(m,z,t) = \int E^{\pm}(m,\omega,z,t)\mathrm{d}\omega$. Likewise, the absence of the ($\pm$) superscript denotes summation over both upward and downward propagating wavefields.

[4]The convention has been taken that both wavenumber and frequency are positive. The direction of propagation or sign of a spatial flux is given explicitly and C_{gz} has been assumed to be positive definite.

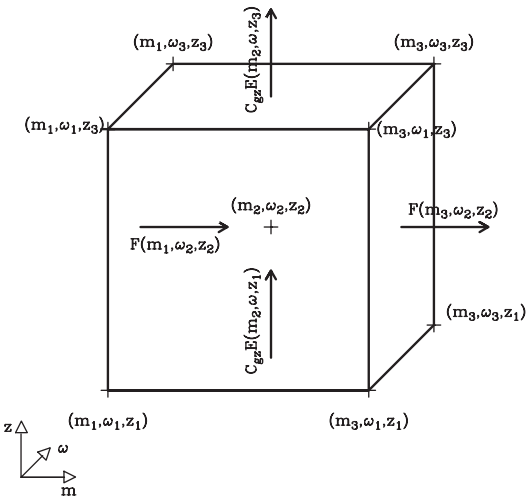

Figure 3. The energy balance for the vertical wavenumber–frequency energy density spectrum, $E(m, \omega, z)$, at vertical wavenumber m_2, frequency ω_2 and vertical coordinate z_2. The vertical flux of energy is $C_{gz}E$. Transports of energy to small scales are represented by F. Transports of energy in the frequency domain, G, are not depicted.

having an $S_o^{\pm}$ representation. Finally, dissipation is viewed as being implicitly represented in (13) as high wavenumber transports F rather than having an explicit $S_i^{\pm}$ representation. Setting the righthand-side of (13) to zero and integrating over the vertical wavenumber, frequency domain; $\int_0^{\infty}\int_f^N dm\, d\omega$; returns:

$$\frac{\partial \hat{E}}{\partial t} + \frac{\partial E_{flux}}{\partial z} = -\int_f^N F_e\,(m=\infty,\omega)\,d\omega\,, \qquad (14)$$

in which no flux boundary conditions have been implemented $F(m = 0, \omega) = 0$, $G(m,\omega = f) = 0$ and $G(m,\omega = N)=0$. Here $\hat{E}$ represents the total energy and E_{flux} the total vertical energy flux. The high wavenumber transport $\int_f^N F_e(m=\infty,\omega)\,d\omega$ is interpreted as representing the rate of dissipation of internal wave energy.

5. A General Formulation

With a zero righthand-side, (13) does not conserve wave momentum. This result can be obtained by multiplying (13) by $k/\beta\omega = \beta(\omega)m$ with $\beta = [(\omega^2 - f^2)/\ \omega^2(N^2-\omega^2)]^{1/2}$ and identifying the downscale transport of wave momentum as $F_p = (k/\omega)F_e$, *etc.* It is, however, possible to construct an $[S_o^{\pm} - S_i^{\pm}]$ representation that serves to conserve momentum while still conserving energy (Polzin, 2001a). The trick is facilitated by realizing that, while energy is positive definite, momentum is a signed quantity. The conservation of momentum can be guaranteed by the backscattering of wave energy into an oppositely signed wavevector at a rate in proportion to the spectral transports so that no net energy is generated or dissipated. In terms of an upward–downward decomposition, a general expression is

$$\frac{\partial E^{\pm}}{\partial t} \pm \frac{\partial\left[C_{gz}E^{\pm}\right]}{\partial z} + \frac{\partial F_e^{\pm}}{\partial m} + \frac{\partial G_e^{\pm}}{\partial \omega} = \frac{1}{2m}\left[F_e^{\mp} - F_e^{\pm}\right] + \frac{1}{2}\frac{\left[G_e^{\mp} - G_e^{\pm}\right]}{\beta}\frac{\partial \beta}{\partial \omega}\,. \qquad (15)$$

Note that the equation for the total energy density $E = E^+ + E^-$ has a zero righthand-side. Thus energy is conserved. Multiplying (15) by $\pm\, k/\omega$, recognizing that $P^{\pm} = \pm\, k\, E^{\pm}/\omega$ and combining terms returns

$$\frac{\partial P}{\partial t} \pm \frac{\partial\left[C_{gz}P\right]}{\partial z} + \frac{\partial F_p}{\partial m} + \frac{\partial G_p}{\partial \omega} = 0\,. \qquad (16)$$

Thus momentum is conserved.

6. Specific Flux Representations

Potential representations for F and G are discussed in Polzin (2001a). Specifically,

$$F^{\pm}(m,\omega) = A m^4 N^{-1} \phi(\omega)\, E^{\pm}(m,\omega) E(m)\,, \qquad (17)$$

with $A = 0.10$ and

$$\phi(\omega) = (\omega^2 + f^2)\left[\left(\omega^2 - f^2\right)\left(N^2 - \omega^2\right)\right]^{1/2} / \left[\omega^2\left(N^2 - f^2\right)\right]; \quad \& \; G^{\pm}(m,\omega) = 0\,. \qquad (18)$$

In (17), $\phi(\omega)$ accounts for the conversion from horizontal to vertical wavenumber and conversion from shear spectral density to energy density by invoking a linear dispersion relation. The specification of $A = 0.10$ renders (17) to be consistent with Polzin *et al.* (1995). Equation (17) represents a *non-local* flux as the transport at vertical wavenumber and frequency (m,ω) is proportional to the shear spectral density integrated over all frequencies.

An expression quite similar to (17) was utilized by Polzin *et al.* (1995) in a model/data validation study. When evaluated at $m = m_c$, and with factors involving wave frequency estimated from the shear–strain ratio, (17) accurately predicts the rate of dissipation of turbulent kinetic energy ε to within a factor of ± 2, the approximate statistical uncertainty of the measurements.

The expression given in (17) was constructed to have the property of relaxing perturbed internal wave spectra back to an m^{-2} power law. This can easily be inferred by realizing that F is non-divergent for such spectra. It was not constructed to produce an m^{-3} saturation regime. This will have little impact on the vertical distribution of momentum and energy flux divergences. With an O~1 non-linear time scale (*c.f.* (11)), waves within the oceanic

saturation regime will dissipate before propagating one vertical wavelength.

With the specification (17), the associated term on the righthand-side of (15) becomes:

$$\frac{1}{2m}[F_e^{\mp} - F_e^{\pm}] = \frac{Am^3\phi(\omega)}{2N}[E^{\mp}(m,\omega) - E^{\pm}(m,\omega)][E^{\pm}(m) + E^{\mp}(m)]. \quad (19)$$

This closely resembles Bragg scattering in the resonant interaction scheme (Polzin, 2001a). It will serve to equilibrate a vertically anisotropic wavefield.

There appears to be little consensus regarding the net frequency domain transports. The null hypothesis of (18) has therefore been put forward. One possible interpretation of (18) is that the internal wavefield does no net work on itself.

7. Discussion

The work presented above describes a method for assessing the spatial and temporal evolution of an internal wave spectrum. This method invokes a mixed spatial/spectral representation that does not invoke a wave packet formulation. This enables the construction of quite general flux representations for nonlinear transports that conserve both momentum and energy. Momentum conservation is attained by transferring energy into an oppositely signed wavevector.

A closure scheme for the spectral transport of energy was also presented. This closure scheme is a simplistic treatment of interactions between internal waves. It contains the following three ingredients: (i) consistency with linear propagation in the absence of non-linearity, (ii) high wavenumber vertical wavenumber domain transports in agreement with an empirically defined transport $F(m_c)$ and (iii) relaxation back to an equilibrium vertical wavenumber spectrum. In the long term, the potential revision of transport laws as dictated by observational studies is envisioned. A more detailed description of this work is presented in Polzin (2001a). Idealized solutions to the governing equation (15) with (17) and (18) are considered in Polzin (2001b).

Acknowledgments: Financial support from the National Science Foundation (Grant No. OCE 94-15589) and the office of Naval Research (Grant No. N00014097-1-0087) is gratefully acknowledged.

References

Cairns, J. L., and G. O. Williams, 1976. Internal wave observations from a midwater float. 2. *J. Geophys. Res.*, **81**, 1943–1950.

Dewan, E. M., N. Gossbard, A. F. Queseda, and R. E. Good, 1984. Spectral analysis of 10 m resolution scalar velocity profiles in the stratosphere. *Geophys. Res. Lett.*, **11**, 80–83.

Dewan, E. M. and R. E. Good, 1986. Saturation and the "universal" spectrum of vertical profiles of horizontal scalar winds in the atmosphere. *J. Geophys. Res.*, **91**, 2742–2748.

Duda, T. F., and C. S. Cox, 1989. Vertical wavenumber spectra of velocity and shear at small internal wave scales. *J. Geophys. Res.*, **94**, 939–950.

Fritts, D. C. and W. Lu, 1993. Spectral estimates of gravity wave energy and momentum fluxes. Part II: Parameterizing of wave forcing and variability. *J. Atmos. Sci.*, **50**, 3695–3713.

Gargett, A. E., P. J. Hendricks, T. B. Sanford, T. R. Osborn, and A. J. Williams III, 1981. A composite spectrum of vertical shear in the ocean. *J. Phys. Oceanogr.*, **11**, 1258–1271.

Garrett, C. J. R. and W. H. Munk, 1975. Space-time scales of internal waves. A progress report. *J. of Geophys. Res.*, **80**, 291–297.

Gregg, M. C., D. P. Winkel, and T. B. Sanford, 1993. Varieties of fully resolved spectra of vertical shear. *J. Phys. Oceanogr.*, **23**, 124–141.

Hines, C. O., 1993. The saturation of gravity waves in the middle atmosphere. Part IV: Cutoff of the incident wave spectrum. *J. Atmos. Sci*, **50**, 3045–3060.

Hines, C. O., 1997. Doppler spread parameterization of gravity wave momentum deposition in the middle atmosphere. Part I: Basic formulation. *J. Atmos. Solar-Terr. Phys.*, **59**, 387–400.

Kunze, E. and T. B. Sandford, 1996. Abyssal mixing: where it isn't. *J. Phys. Oceanogr.*, **26**, 2286–2296.

Lindzen, R. S., 1981. Turbulence and stress owing to gravity wave and tidal breakdown. *J. Geophys. Res.*, **64**, 9707–9714.

Müller, P., G. Holloway, F. Henyey and N. Pomphrey, 1986. Nonlinear interactions among internal gravity waves. *Rev. Geophys.*, **24**, 493–536.

Munk, W., Internal waves and small-scale processes, In: Evolution of Physical Oceanography, B.A. Warren and C. Wunsch, Eds., The MIT Press, Cambridge, 264–291, 1981.

Polzin, K. L, 1999. A rough recipe for the energy balance of quasi-steady internal lee waves. In: *Internal Wave Modeling*, Peter Müller and Diane Henderson, editors. Proceedings, Hawaiian Winter Workshop, University of Hawaii at Manoa, January 19–22, 1999; Hawaii Institute of Geophysics, Special Publication.

Polzin, K. L., 2001a. On flux representations of internal wave spectral transports. *J. Mar. Res.*, submitted.

Polzin, K. L., 2001b. Idealized solutions for the energy balance of the finescale internal wave field. *J. Mar. Res.*, submitted.

Polzin, K. L., J. M. Toole, and R. W. Schmitt, 1995. Finescale parameterizations of turbulent dissipation. *J. of Phys. Oceanogr.,* **25**, 306–328.

Polzin, K. L., 1996. Statistics of the Richardson number: Mixing models and fine structure. *J. of Phys. Oceanogr.,* **26**, 1409–1425.

Polzin, K. L., J. M. Toole, J. R. Ledwell, and R. W. Schmitt, 1997. Spatial variability of turbulent mixing in the abyssal ocean. *Science*, **276**, 93–96.

Smith, S. A., D. C. Fritts, and T. E. Van Zandt, 1987. Evidence for a saturated spectrum of atmospheric internal gravity waves. *J. Atmos. Sci.*, **44**, 1404–1410.

Toole, J. M., K. L. Polzin, R. W. Schmitt, 1994a. Estimates of diapycnal mixing in the abyssal ocean. *Science*, **264**, 1120–1123.

Van Zandt, T. E. and D. C. Fritts, 1989. A theory of enhanced saturation of the gravity wave spectrum due to increases in atmospheric stability. *Pure Appl. Geophys.*, **130**, 399–420.

Wu, Y. F. and H. U. Widdel, 1991. Observational evidence of a saturated gravity wave spectrum in the mesosphere. *J. Atmos. Terr. Phys.*, **51**, 991–996.